The Study of Tailings at Mina Alumina Limited, Mozambique.

Quiven. I. Ebicha[1], Amadeu C. dos Muchangos[2] and Hernâni V. Nhatinombe[3]
1. Undergraduate student in Applied Geology
2. Senior lecturer
3. Assistant lecturer
Department of Geology, Faculty of Sciences, Eduardo Mondlane University, Maputo, Mozambique
Corresponding author: quiven89@gmail.com

Abstract

The beneficiation of gibbsite at their washing plants is one of the most important processes at Mina Alumina Limited in Mozambique. During this operation, large volumes of tailings are produced. Since the company started operating in this region in the early decades of the 20th century, only a few geologists, mining engineers and environmental scientists have studied the material in these tailings deposits. This paper summarises observations and measurements made in one of the inactive Mina Alumina tailings deposits. The deposit was divided into three sections and samples were collected for laboratory studies. Pycnometry was used to determine the density variation of the solids around of the deposit. X-Ray Diffraction was used to determine the mineralogical composition and for phase quantification. Chemical analysis was by Graphite Furnace Atomic Absorption Spectrometry (GFAAS) and Flame Atomic Absorption Spectrometry (FAAS). Through the graphs constructed after grain size analysis, it was possible to demonstrate the variation of the Fineness Modulus, Curvature Coefficient, Uniformity Coefficient and the variation of permeability around the deposit. Studies of these tailings are important in informing future options for reuse of the material and facilitating studies of their environmental impacts.

Keywords: Penhalonga, Mina Alumina Limited, Gibbsite, Tailings, Tailings' deposit.

1. Introduction

Mina Alumina Limited is a bauxite mining and processing company operating on the Penhalonga Mountain in the Province of Manica, Mozambique. It was the first mine to be owned by an individual or organisation from outside Mozambique, having operated since 1935 and is presently the only bauxite mine operating in Southern Africa. Production was carried out continuously until 1974 and during that period roughly 4 000 tonnes of ore per annum were mined for the manufacture of aluminum sulphate and refractory bricks. After an interruption of 10 years, production was resumed in 1985 and until the beginning of the 1990s about 6 000 tonnes per annum were extracted from seven quarries [1].

1.2. Geological Setting of the Bauxite Deposits of Penhalonga

The bauxite deposits occur in the northern margin of the Precambrian greenstone belt in Manica Province, and extends along the Mozambique - Zimbabwe border at altitudes ranging from 800 to 1 800 metres.

This Precambrian unit is built up of Archean and Proterozoic, as well as Phanerozoic magmatic and metamorphic rocks. The laterite-bauxite blanket overlies mainly basement Precambrian gabbros, anorthosites, diorites, granites and metamorphosed basic volcanic rocks. The ore bodies, of residual character, overlie gabbro-anorthositic rocks, metabasalts, talcschist and also granite.

The deposit is part of the South-East African Province of lateritic bauxites [2]. The total area of the deposit has approximately 1 600 hectares [3].

1.3. Reserves

The deposit's bauxite reserves were initially evaluated in 1963, at 600 000 tons, but in 1994, the reserves were revaluated with the support of the United Nations Development Program (UNDP) at 1 374 000 tonnes. Up to the end of 2017 about 112 000 tons were extracted leaving approximately 1 262 000 tonnes, which can be mined for at least 105 years assuming 2017 levels of production [3]. The different ore grades extracted and processed at Mina Alumina Limited are used mainly for the manufacture of aluminum sulphate used in water purification.

1.4. The Grades and Distribution of Ore Bodies

According to the principal petrographic and chemical characteristics, four main ore types/grades can be defined, and their chemical analyses are presented in Table 1.

Table 1. Chemical composition of representative ore types from the Penhalonga deposit [1].

Oxide (wt %)	**Ore type A**	**Ore type B**	**Ore type C**	**Ore type D**
Al_2O_3	58.43	49.65	44.02	57.16
Fe_2O_3	1.55	13.81	17.78	0.64
TiO_2	0.27	0.84	3.07	0.00
SiO_2	9.0	9.19	9.92	16.92
L.O.I.	28.62	23.9	24.12	24.03
Na_2O	0.04	0.04	0.07	0.11
K_2O	1.65	1.20	0.10	0.58
CaO	0.02	0.08	0.00	0.03
MgO	0.27	0.09	0.00	0.00
P_2O_3	0.01	0.04	0.21	0.02
MnO	0.06	0.03	0.07	0.06
Total	99.92	98.93	99.36	99.57

The main characteristics of the ore types are as follows:

Type A: White saprolitic bauxite, friable, texturally porous and light. Primary parent rock structures, notably joints and fractures, are often preserved. It is related to anorthosites.

Type B: Yellowish brown saprolitic bauxite presenting similar characteristics as grade A. It is related to the intermediate members of the gabbro/anorthosite series.

Type C: Reddish brown to dark brown, ferruginous, saprolitic bauxite. Fine grained, friable, but also indurated in some places, with lateritic appearance showing ferruginous cement. It is related to the metabasalts.

Type D: White kaolinitic clays, with concretionary, collomorphic gibbsite. The contents of gibbsite nodules are very variable and so are their sizes and shapes. The clay is sticky when wet and extremely fine and friable when dry. It is also related to anorthosites.

1.5. Gibbsite Beneficiation

The gibbsite nodules contained in the type D ore are beneficiated at the washing plants to separate them from the kaolinitic clays, residual bauxite, and other impurities. After separation, the gibbsite nodules are carried straight to the processing plant where they are crushed and later mixed with the type C ore to improve the quality of that ore. The kaolinitic clays and the other material, all considered waste products, are transported to the tailings deposits. The main objective of this paper is to present the main characteristics of the tailings present in the deposit, and to suggest applications for this material.

2. Sampling and Analytical Measurements

The tailings deposit from which the samples were collected was divided into three sections (A, B and C) according to Figure 1. This was necessary because the distribution of the particle grains varies around the tailings deposit in a roughly semicircular pattern from the discharging point.

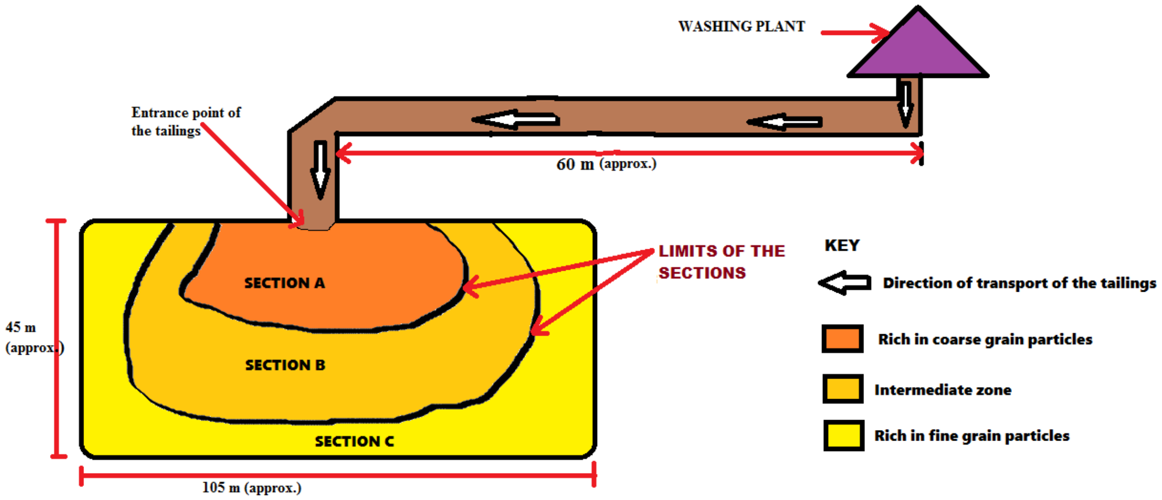

Figure 1. Sketch showing the divisions made on the surface of the tailings deposit during sample collection.

Sample preparation was carried out in the Sample Preparation Laboratory of the Department of Geology of the Eduardo Mondlane University. This step involved the elimination of organic matter contained in the samples using hydrogen peroxide (H_2O_2) and grinding using a Herzog grinder. The samples were dried at 60 °C using the WTC Blinder dryer.

2.1. Pycnometry

Pycnometry was used to determine the solids density variation around the deposit. The liquid used was xylene (ortho, meta and para-dimethyl benzene isomeric mixture) since it has a constant and known density and temperature relationship. The xylene had the following main properties: Density at 20 °C = 0.866 g / cm^3, temperature stabilised to 20 °C and percentage of water $\leq 0.03\%$. The formula used to calculate the approximate densities is shown in equation 1:

$$D = \frac{M2-M1}{(M4-M2)-(M3-M2)} \tag{1}$$

Where:

D Density of the solid part;
M1 Mass of the pycnometer;
M2 Mass of the pycnometer + sample;
M3 Mass of the pycnometer + sample + xylene;
M4 Mass of the pycnometer + xylene

2.2. Wet and Dry Sieving

These methods were used for size distribution analysis. The wet sieving was performed manually using the nº 325 sieve (0.045 mm) to separate and measure fine and coarse particles. The dry sieving was performed mechanically for 15 minute continuous vibration intervals, using a PTT TAMSON - Zooetermer Holland vibrator to determine the size characteristics; Curvature coefficient (CC) and Coefficient of Uniformity (CU). The Permeability and the Fineness Modulus (FM) was also determined. The formulas of the grading characteristics are presented in equations 2 and 3, while equation 4 was used to calculate the permeability.

$$CU = \frac{D60}{D10} \tag{2}$$

Where:

CU	Coefficient of Uniformity
D60 and D10	Grain diameters, in millimeters, known as effective size corresponding to 60% finer by weight and 10% finer by weight respectively.

$$CC = \frac{D30\ x\ D30}{D60\ x\ D10} \tag{3}$$

Where:

CC	Coefficient of curvature
D10, D30 and D60	Grain diameters, in mm, corresponding to 10, 30 and 60% finer by weight respectively.

$$K = CD_{10}^{2} \tag{4}$$

Where:

K	Permeability
D10	Effective grain diameter corresponding to 10% finer by weight obtained from the grain size distribution curve
C	Coefficient that can be considered equal to 0.01.

2.3. X-ray Diffraction (XRD)

Analysis was carried out using an OLYMPUS BTX 525 diffractometer. The interpretation of the diffractograms to identify the minerals present was carried out using the XPowder Version 2010.01.35.PRO. A total of 8 samples being 3 from section A (SA-1, SA-2 and SA-3), 3 from section B (SB-1, SB-2 and SB-3) and 2 from section C (SC-1 and SC-2) were analyzed.

2.4. Graphite Furnace Atomic Absorption Spectrometry (GFAAS) and Flame Atomic Absorption Spectrometry (FAAS)

These methods were used to quantify the major and trace elements present in the samples collected from the same tailings deposit in 2010. The experiments were carried out in the analytical chemistry laboratory at the Department of Chemistry of the Eduardo Mondlane University [4].

3. Results

3.1. Pycnometry

Table 2 shows the results obtained after calculating the approximate densities using equation 1.

Table 2. The approximate density intervals.

Sample Section	Intervals of the approximate densities
A	3.92 to 4.24 g / cm^3.
B	2.42 to 2.64 g / cm^3
C	2.16 to 2.61 g / cm^3.

3.2. Wet sieving

Table 3 shows the final weights including the percentages of the coarse fraction (retained in the nº 325 sieve) and the fine fraction (which passed the nº 325 sieve).

Table 3. Final masses and percentages of the coarse and fine fractions.

Section	Tare + Sample (g)	Coarse fraction		Fine fraction	
A	268.704	96.816 g	48.4%	92.027 g	46.0%
B	198.395	29.167 g	14.5%	134.465 g	67.2%
C	207.035	21.817 g	10.9%	158.822 g	79.3%

3.3. Dry Sieving

Tables 4, 5 and 6 show the weight distribution of the size fractions and their respective percentages (retained and passing) and their respective curves on Figures 2, 3 and 4.

Table 4. Grain size distribution of sample collected from section A.

Sample from Section A							
Sieve number	Grain diameter		Weight Retained (g)	Weight Retained (%)	Cumulative weight retained (%)	Weight Passing (g)	Cumulative weight passing (%)
	mm	µm					
18	1.000	1000	13.46	13.90	13.90	83.36	86.10
25	0.710	710	12.57	12.98	26.88	70.79	73.12
35	0.500	500	19.20	19.83	46.71	51.58	53.29
45	0.355	355	10.91	11.26	57.97	40.68	42.03
60	0.250	250	20.97	21.66	79.63	19.71	21.37
80	0.180	180	5.63	5.82	85.45	14.08	14.55
120	0.125	125	0.47	0.49	85.94	13.61	14.06
200	0.075	75	5.90	6.10	92.04	7.71	7.96
230	0.063	63	5.59	5.77	97.81	2.12	2.19
Pan	< 0,063	< 63	2.12	2.19	100		

Table 5. Grain size distribution of sample collected from section B.

Sample from Section B							
Sieve number	Grain diameter		Weight retained (g)	Weight retained (%)	Cumulative weight retained (%)	Weight Passing (g)	Cumulative weight passing (%)
	mm	µm					
18	1.000	1000	0.30	1.02	1.02	28.87	98.98
25	0.710	710	5.06	17.36	18.38	23.80	81.62
35	0.500	500	4.10	13.98	32.36	19.72	67.64
45	0.355	355	2.93	10.05	42.41	16.79	57.59
60	0.250	250	3.31	11.36	53.77	13.47	46.23
80	0.180	180	2.69	9.22	62.99	10.80	37.01
120	0.125	125	0.14	0.49	63.48	10.65	36.52
200	0.075	75	5.36	18.37	81.85	5.30	18.15
230	0.063	63	3.76	12.89	94.74	1.53	5.26
Pan	< 0.063	< 63	1.53	5.26	100	-	-

Table 6. Grain size distribution of sample collected from section C.

Sample from Section C							
Sieve number	**Grain diameter**		**Weight retained (g)**	**Weight retained (%)**	**Cumulative weight retained (%)**	**Weight passing (g)**	**Cumulative weight passing (%)**
	mm	**µm**					
18	1.000	1000	0.18	0.83	0.83	21.64	99.17
25	0.710	710	1.97	9.05	9.88	19.66	90.12
35	0.500	500	2.71	12.41	22.29	16.96	77.71
45	0.355	355	1.89	8.66	30.95	15.07	69.05
60	0.250	250	1.62	7.44	38.39	13.44	61.61
80	0.180	180	0.36	1.66	40.05	13.08	59.95
120	0.125	125	1.84	8.44	48.49	11.24	59.51
200	0.075	75	6.24	28.61	77.1	4.99	22.9
230	0.063	63	2.54	11.64	88.74	2.46	11.26
Pan	< 0.063	< 63	2.46	11.26	100	-	-

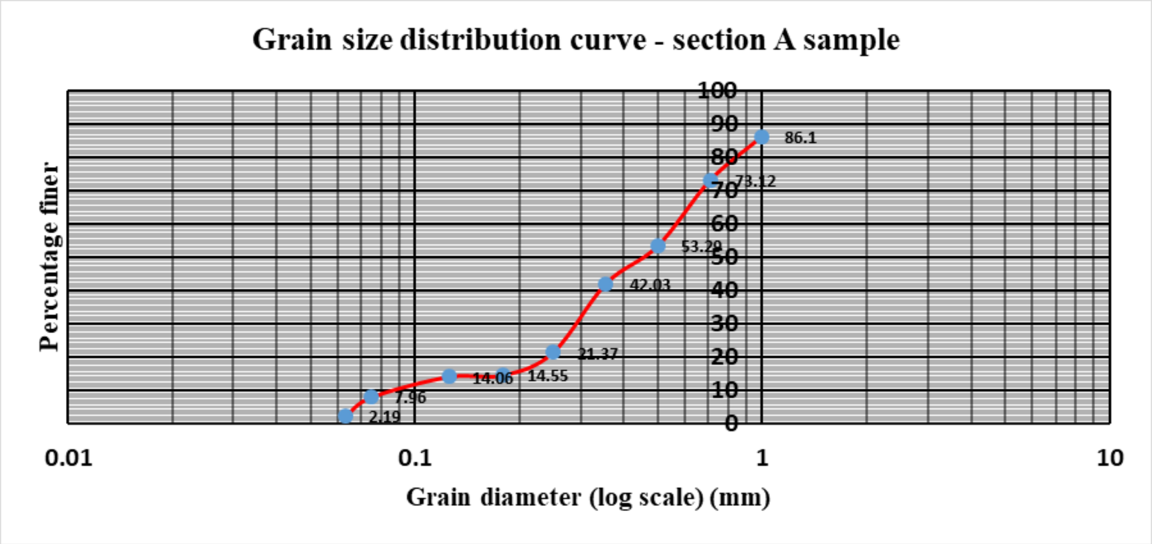

Figure 2. Grain size distribution curve of sample from section A.

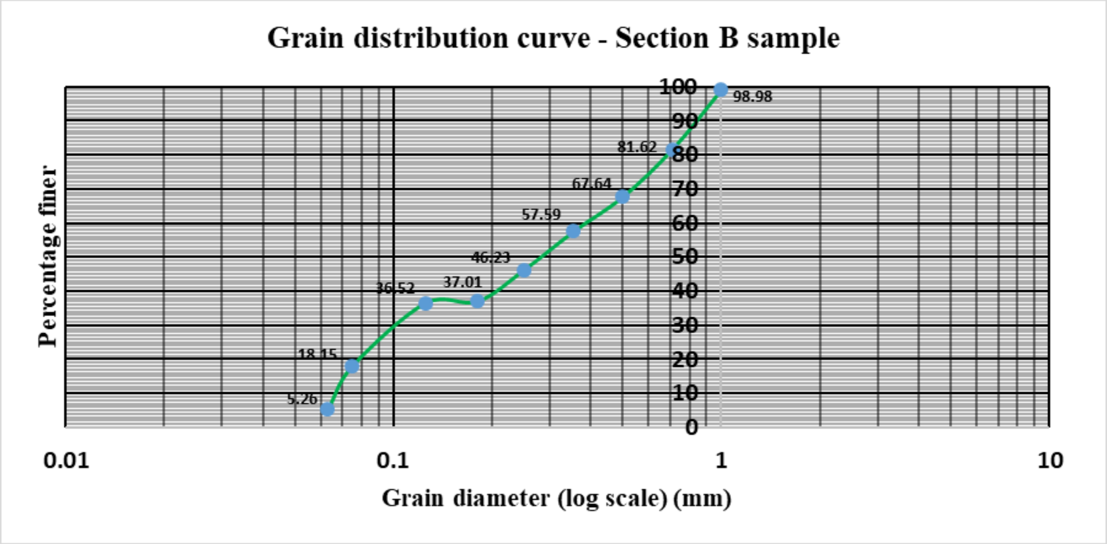

Figure 3. Grain size distribution curve of sample from section B.

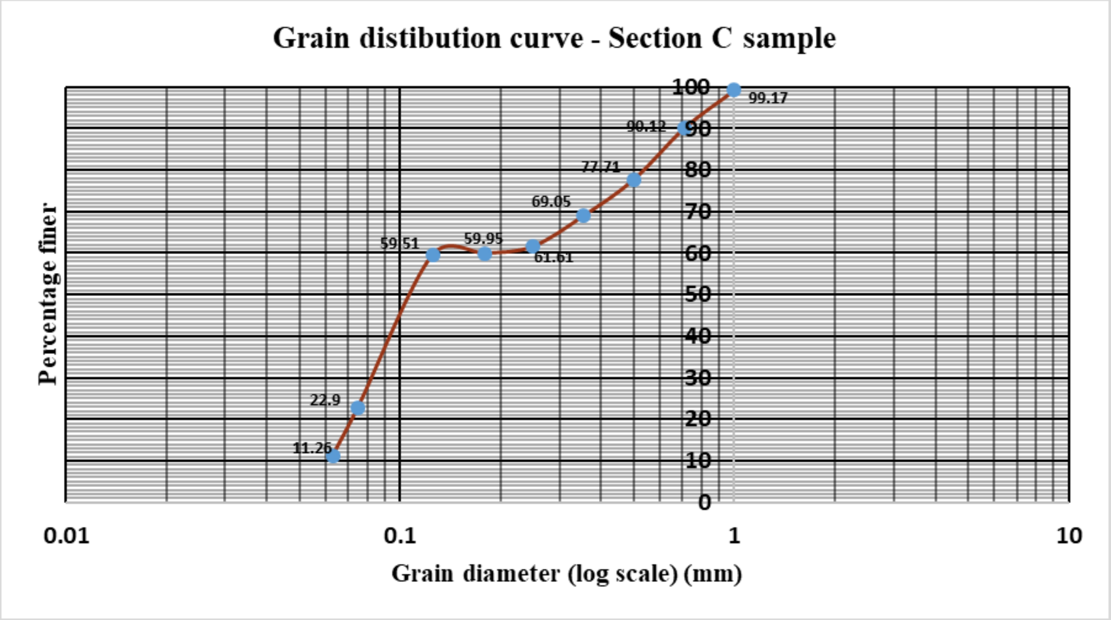

Figure 4. Grain size distribution curve of sample from section C.

Table 7 shows the results obtained from calculating the fineness modulus (FM), curvature coefficient (CC), coefficient of uniformity (CU) and permeability (K).

Table 7. Fineness Modulus Values, Curvature Coefficient, Coefficient of Uniformity and Permeability.

Sample's section	Fineness modulus	Curvature coefficient	Coefficient of uniformity	Permeability (cm/s)
A	6.86	1,64	6,3	8×10^{-7}
B	5,51	0,4	5,92	4.2×10^{-7}
C	4,57	?	?	?

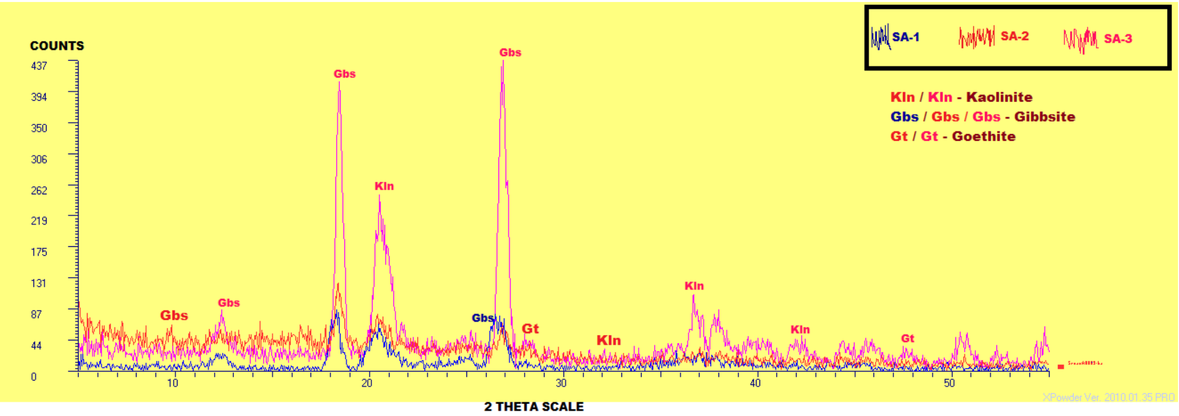

Figure 5. X-ray diffraction pattern of tailings sample SA-1, SA-2 and SA-3.

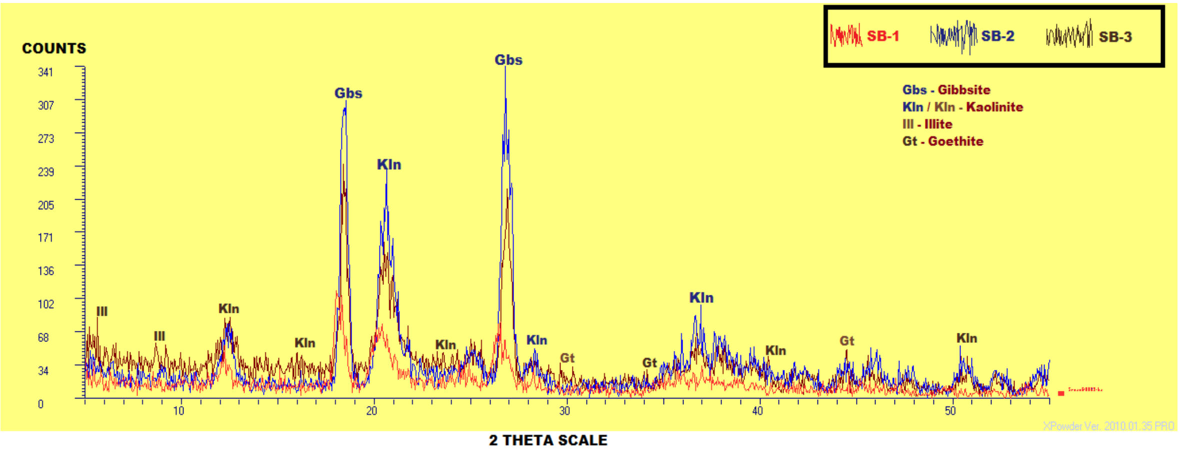

Figure 6. X-ray diffraction pattern of tailings sample SB-1, SB-2 and SB-3.

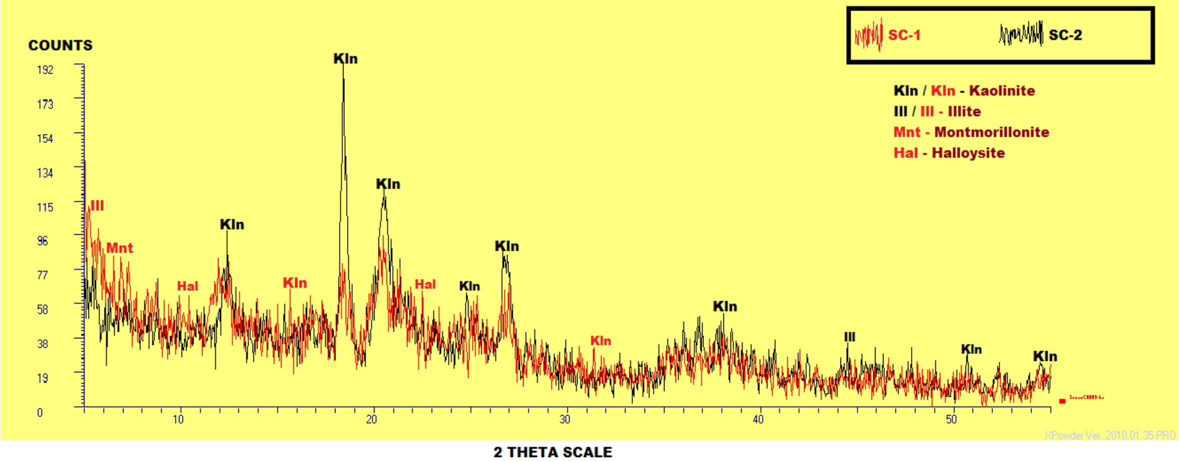

Figure 7. X-ray diffraction patterns for tailings samples SC-1 and SC-2.

3.4. X-ray Diffraction

Figures 5 to 7 show the diffractograms obtained from the mineralogical analysis of the samples collected from sections A, B and C respectively.

3.5. Chemical Analysis

Table 8 presents the major elements measured in the Mina Alumina Limited tailings after the beneficiation of gibbsite nodules obtained in 2010.

Table 8. Results of the chemical analysis of major elements. [4]

Oxide	Sample 1 (%)	Sample 2 (%)	Average (%)
Al_2O_3	36.10	36.30	36.20
Fe_2O_3	2.80	2.74	2.76
SiO_2	39.60	39.94	39.77
TiO_2	0.123	0.12	0.012
MnO	0.02	0.02	0.02
MgO	0.79	0.80	0.80
CaO	< 0.0014	< 0.0014	-
Na_2O	0.32	0.312	0.32
K_2O	0.46	0.46	0.47
P_2O_5	0.01	0.01	0.01

Table 9 presents the trace elements measured in the tailings in 2010.

Table 9. Results of the chemical analysis of the trace elements. [4]

Trace element	Sample 1 (ppm)	Sample 2 (ppm)	Average (ppm)
Ba	71.20	77.30	77.25
Cr	54.80	57.90	56.35
Cu	42.30	43.10	42.70
Ni	24.50	24.00	24.25
Pb	11.10	10.20	10.65
Sr	5.40	5.60	5.50
V	32.20	22.40	27.30
Zn	21.30	20.80	21.05
Zr	5.80	7.20	6.50

4. Discussion

According to the results in table 2, the approximate density of the solids in the tailings' deposit ranges from 2.16 to 4.24 g/cm^3. The solids from section A are the densest, ranging from 3.92 to 4.24 g/cm^3. The density of the solids in the deposit decreases from the discharge point towards the edges of the deposit. The presence of goethite, an iron mineral, in samples SA-2 and SA-3 would have contributed to the high density. The solids in section C are the least dense, varying from 2.16 to 2.61 g/cm^3 and this may be due to the predominance of light clay minerals.

Through the results presented in Table 3, section A contains the lowest quantity of fine clay particles and the highest quantity of coarse particles, whereas the opposite is observed in Section C. This is because where the tailings are discharged, the coarse fraction tends to settle around that point (the case of section A), while the fines particles tend reach long distances, due to the decrease of the particle size and density (observed in sections B and C, respectively). Therefore many tailings' deposits are considered to be heterogeneous because the layers formed usually vary in thickness and particle size distribution, and such phenomenon is verified along the vertical section of the deposit. As far as the vertical distribution is concerned, two types of sediments are distributed in the form of intercalated layers (laminar layers of very fine clay particles alternating with layers of coarse particles). Coarse particles are denser than fine clay particles and tend to decant as soon as they are introduced into the tailings' deposit while those of clays remain suspended in the pulp, only settling with time, or when the washing plant is switched off. In other words the deposition of the coarse grains tend to occur horizontally or obliquely while the deposition of the very fine clay particles which remain in suspension tend to occur vertically [5].

The dry sieving results show that approximately 86 % of the particles have a diameter greater than 0.075 mm. The quantity of the particles contained in sections B and C, and whose diameters are above 0,075 mm, are 63.48 % and 48.49 % respectively. Once again, this shows that the amount if coarse particles reduces as we move away from the discharge point. This can be also sustained by the results of the fineness modulus shown in table 7 which reveal that section A of the tailings deposit, whose value is 6.86 and the highest, is composed of coarser particles relative to sections B and C (5.51 and 4.57 respectively). The fineness modulus is an empirical factor obtained by adding the cumulative percentages of aggregate retained on each sieve and dividing the sum by 100. The standard sieves ranging from 80 mm to 150 μm are those used in the civil construction industry, but in the present study the fineness modulus was only used to specify the variation of the grain size distribution along the tailings deposit with sieves ranging from 1 mm to 63 μm. The fineness modulus variation can be considered as a convenient means of keeping quality history data on uniformity of particle-size distribution of aggregate production, delivery and use. This factor can be also important because some agencies require that aggregates be processed to remain within upper and lower limits of fineness modulus.

Permeability is also affected by the grain size distribution. According to the results in Table 7 the particles contained in sections A and B can be considered as non-plastic mud or of low plasticity [5], since the permeability values obtained were 8 x 10^{-7} cm/s and 4.2 x 10^{-7} cm/s respectively. The permeability of the tailings contained in section C was not specified due to the difficulty in obtaining the D10 value from the grain size distribution curve. These particles can be inferred as high plasticity muds because this section of the tailings' deposit is composed mainly of clay particles whose diameter is less than 0.045 mm (see Table 3). The void ratio also controls the permeability and it decreases as the distance from the point of discharge of the tailings into the deposit increases. The void ratio also decreases as the depth increases due to the weight of the overlying material.

As far as the grading characteristics of the tailings (Table 7) are concerned, the grains contained in section A can be classified as well graded (the particles are distributed over a wide size range) with a CU value of 6.3 and the curvature coefficient is 1.64. For the soil to be well graded, the value of CU must be greater than 4 and CC should be in the range of 1 to 3 [6]. So, the higher the value of CU the larger the range of the particle sizes in the tailings. The value of CU for tailings contained in section B is approximately 5.92 and the CC value is 0.4 which means that they can be considered as gap graded due to the value of CC, which is out of the specified and standardized range.

Most gap graded soils have CC outside the standardized range, and this can be due to the absence of intermediate particle sizes; for the case of the section B sample which was analyzed, this can be due to the small percentage of the weight retained in the nº 120 sieve (0.49 %), seenin the almost flattened part of the grain size distribution curve. It was not possible to calculate the grading characteristics for the section C sample due to the lack of the D10 values, but through analyzing the similarities of the grain size distribution curve with that of the Section B, it is possible to consider the tailings from this section as gap graded. The grain size analysis of these tailings has a very important practical significance as far as their areas of application are concerned. Grain size distributions larger than 0.075 mm have several important uses. They affect the void ratio and may provide useful information for use in cement and asphaltic concretes. Well graded aggregates require less cement per unit of volume of concrete to produce denser, less permeable concrete, and more resistance to weathering because if the tailings are well-graded, the void ratio should be less [6]. The percentage of fines and the gradation of coarse particles in the tailings may also be useful in making a choice of material for the base course under highways, runways and rail tracks to give a mechanically stable foundation to the loads coming on to the pavement [6]. In the case of earth dam constructions, different gradations are required in the different zones of the construction. The Section A particles can also become useful in this case as the fill material because certain type of constructions are required to have well-graded materials which contribute to its strength. Grain size distribution of tailings smaller than 0.075 mm may be of little importance in engineering solutions but may be useful in making molded cups, vases, statues and plates.

X-Ray diffraction analysis reveals that kaolinite is the principal mineral present in the tailings deposit and was detected in the 8 samples analyzed. The other clay minerals detected by this method were illite (samples SB-3 and SC-1), montmorillonite (sample SC-1) and halloysite (sample SC-1). These four clay minerals can occur in an intermixed form in bauxites deposits. Gibbsite was the second principal mineral detected especially in samples collected from sections A and B, revealing that not all particles of this mineral are retained by the vibrating screen during beneficiation. Goethite was also detected in the samples from sections A and B. Table 10 shows the recalculated percentages of the main crystalline constituents of the 8 samples presented on the diffractograms. Knowing these mineralogical compositions is of great importance, for example, in the recovery of gibbsite or any other mineral in future using methods such as froth flotation, which is becoming more widely applied for recovering minerals from residues produced by beneficiation.

Table 10. Semi-quantitative mineral abundances (wt %) determined by DRX .

Mineral	**SA-1 (%)**	**SA-2 (%)**	**SA-3 (%)**	**SB-1 (%)**	**SB-2 (%)**	**SB-3 (%)**	**SC-1 (%)**	**SC-2 (%)**	**AVG. (%)**
Gibbsite	48.8	52.1	52.3	33.4	37.3	-	-	-	27.99
Kaolinite	51.2	43.2	41.6	55.4	56.8	82.2	86.2	91.1	63.46
Goethite	-	4.7	6.1	5.4	-	6.7		-	2.86
Halloysite	-	-	-	-	-	-	3.1	2	0.64
Illite	-	-	-	5.8	5.9	11.1	8.4	6.9	4.76
Montmorillonite	-	-	-	-	-	-	2.3	-	0.29

From the results in table 8, the main major elements detected in the samples analyzed are silicon, aluminum and iron, whose average percentages (as SiO_2, Al_2O_3 and Fe_2O_3 equivalents) are 39.77 %, 36.20 % and 2.76 % respectively. Comparing these results with the XRD analyses it can be concluded that silicon, aluminum and iron are contained mainly in kaolinite, gibbsite and goethite respectively.

Three main groups of trace elements are present in the tailings. The first group is composed of barium and strontium, the second contains chromium, copper, zircon and nickel and the third is zinc, vanadium and lead. These groups are geochemically correlated and may have resulted from the same geological formation processes. This is shown in Figure 8 on the dendrogram created using Minitab 18. From these groupings, the similarity of the second and third group is greater than that of barium and strontium, making it easier to conclude that the elements of these two groups may also be geochemically correlated. This can be observed on the loading plot in Figure 9 where the elements from the second and third group are strongly influenced by the first component.

The detected concentrations of these trace elements don't present a toxicity risk. The Cu and Ni concentrations must always be controlled because they may lead to toxicity of soils and ground water if they become too high. Soil contamination with nickel has a potential negative impact on plants, microorganisms and animals [7]. The high concentrations of Cr, Ni, Cu, Zn and Pb observed (see Table 9) can be attributed to the organic matter from the dense vegetation surrounding the tailings deposit. The organic matter interacts with the trace metals, probably due to the formation of stable complexes, which are adsorbed onto the solid organic matter followed by sedimentation [4].

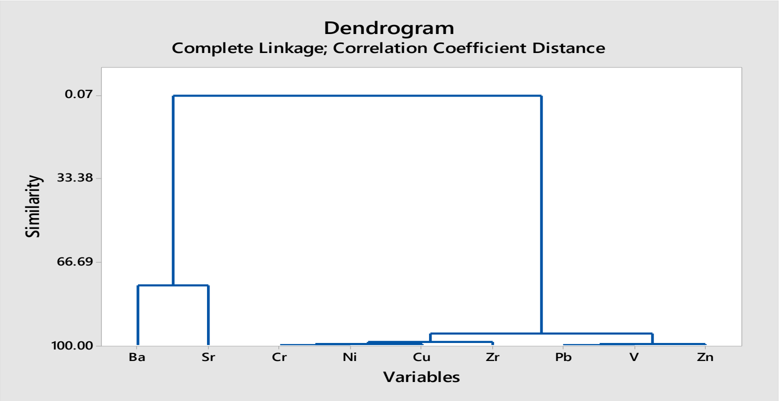

Figure 8. Dendrogram showing the levels of similarity of the trace elements.

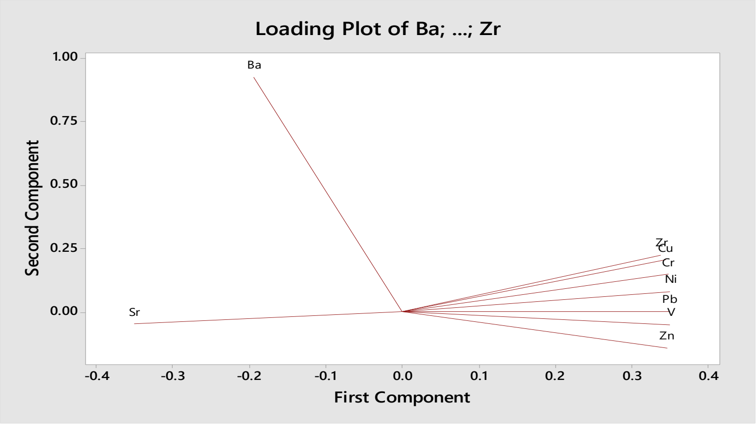

Figure 9. Loading plot showing the association of the trace elements analyzed.

5. Conclusions

During gibbsite beneficiation at Mina Alumina Limited a large volume of residue is produced and transported to the tailings deposit. The tailings deposit studied was divided into three sections and through laboratory analysis it was observed that the grain size distribution is not uniform in particle size, density and mineralogy. Section A, which is closest to the discharge point, contains coarse particles whose deposition occurs almost horizontally or obliquely, while very fine clay particles whose deposition occurs almost vertically, predominate in section C.

The particles from section A are the densest, with density decreasing with distance from the discharge point. The well graded tailings in section A may have application in civil engineering due to their wide size range. Kaolinite is the most abundant mineral in the tailings, detected in all 8 samples analyzed. Gibbsite was also detected in considerable quantities in samples from section A and B, obviously passing the washing plant's vibrating screen. Through the levels of similarity observed by dendrogram analysis, three groups of trace elements were distinguished, revealing their geochemical correlation. The trace element concentrations analyzed do not represent levels of toxicity to the neighboring soils and ground water, but should continue to be monitored. Further investigations are foreseen concerning the actual contents/concentrations of rare trace elements accompanying bauxite formation.

6. Acknowledgements

The authors would like to thank Mina Alumina Limited for permission to collect samples and to carry out the other activities necessary in their operations. They would also like to thank the Department of Geology in the Faculty of Science at the Eduardo Mondlane University for facilitating sample transportation and preparation and the analyses carried out in their laboratories. The authors would also like to thank the Department of Chemical Engineering in the Faculty of Engineering at Eduardo Mondlane University for providing the pycnometers and other apparatus used in the laboratory, and finally to Professor Lopo Vasconcelos for review and corrections of the paper.

7. References

1. A.C. Muchangos**.** Mineralogy and Geochemistry of Bauxite and Bentonite deposits from Mozambique. Utrecht University, Utrecht, Netherlands. 2000. 28 - 30.
2. G. Bardossy; G.J.J. Aleva. Lateric bauxites. *Development in economic geology*, 27. Amsterdam; New York: Elsevier, 1990. 624.

3. Plano de lavra e Viabilidade Económica. Pedido de Prorrogação da Concessão Mineira Nº 8C. Projecto para exploração de Bauxite. Mina Alumina Limitada. 2017. Pages. 18.
4. O.H. Cabral. Estudo dos elementos-traço nas águas, argilas e poeiras resultantes do processamento das bauxites de Manica. Scientific project. Department of Geology, Faculty of Sciences, Eduardo Mondlane University. Maputo. 2010. 4-6, 43.
5. A.B. LUZ, et al. A. Tratamento de Minérios. *Centro de Tecnologia Mineral (CETEM)*. Ministry of Science and Technology. Rio de Janeiro. Brazil. 2010. 831 – 847.
6. B.S.V. VISWANADHAM. Soil mechanics. Department of Civil Engineering. Indian Institute of Technology, Bombay, India. 1-5, 8-15.
7. P.S. HOODA. Trace elements in soils. School of Geography, Geology and Environment. Kingston University. London, UK. 2010. 449, 470.